Neurobiology of Aging 73 (2019) 123–134

Contents lists available at ScienceDirect

Neurobiology of Aging

journal homepage: www.elsevier.com/locate/neuaging

Unveiling the olfactory proteostatic disarrangement in Parkinson's disease by proteome-wide profiling

Mercedes Lachén-Montes [a,b], Andrea González-Morales [a,b], Ibon Iloro [c], Felix Elortza [c], Isidre Ferrer [d], Djordje Gveric [e], Joaquín Fernández-Irigoyen [a,b,1], Enrique Santamaría [a,b,*,1]

[a] Clinical Neuroproteomics Group, Navarrabiomed, Complejo Hospitalario de Navarra (CHN), Universidad Pública de Navarra (UPNA), IdiSNA, Pamplona, Spain
[b] Proteored-ISCIII, Proteomics Unit, Navarrabiomed, Complejo Hospitalario de Navarra (CHN), Universidad Pública de Navarra (UPNA), IdiSNA, Pamplona, Spain
[c] Proteomics Platform, CIC bioGUNE, CIBERehd, ProteoRed-ISCIII, Bizkaia Science and Technology Park, Derio, Spain
[d] Institut de Neuropatologia, IDIBELL-Hospital Universitari de Bellvitge, Universitat de Barcelona, L'Hospitalet de Llobregat, CIBERNED, Spain
[e] Centre for Brain Sciences, Imperial College London, London, UK

ARTICLE INFO

Article history:
Received 7 February 2018
Received in revised form 3 September 2018
Accepted 14 September 2018
Available online 25 September 2018

Keywords:
Parkinson's disease
Olfactory bulb
Proteomics
Systems biology

ABSTRACT

Olfactory dysfunction is one of the earliest features in Lewy-type alpha-synucleinopathies (LTSs) such as Parkinson's disease (PD). However, the underlying molecular mechanisms associated to smell impairment are poorly understood. Applying mass spectrometry–based quantitative proteomics in postmortem olfactory bulbs across limbic, early-neocortical, and neocortical LTS stages of parkinsonian patients, a proteostasis impairment, was observed, identifying 268 differentially expressed proteins between controls and PD phenotypes. In addition, network-driven proteomics revealed a modulation in ERK1/2, MKK3/6, and PDK1/PKC signaling axes. Moreover, a cross-disease study of selected olfactory molecules in sporadic Alzheimer's disease (AD) cases revealed different protein derangements in the modulation of secretagogin (SCGN), calcyclin-binding protein (CACYBP), and glucosamine 6 phosphate isomerase 2 (GNPDA2) between PD and AD. An inverse correlation between GNPDA2 and α-synuclein protein levels was also reflected in PD cerebrospinal fluid. Interestingly, PD patients exhibited significantly lower serum GNPDA2 levels than controls (n = 82/group). Our study provides important avenues for understanding the olfactory bulb proteostasis imbalance in PD, deciphering mechanistic clues to the equivalent smell deficits observed in AD and PD pathologies.

1. Introduction

Olfactory dysfunction is present in up to 95% of patients with Parkinson's disease (PD) (Attems et al., 2014; Doty, 2012b). In Lewy body diseases (LBDs), including PD, the olfactory deficit is an early prodromal event being considered as a premotor sign of neurodegeneration (Baba et al., 2012; Beach et al., 2009; Doty, 2008, 2012b). The initial induction of α-synuclein misfolding and subsequent deposition probably occurs in the olfactory bulb (OB) and/or the enteric nervous system (Klingelhoefer and Reichmann, 2015; Rey et al., 2016). Clinical features of olfactory dysfunction have been correlated with the presence of Lewy-type alpha-synucleopathy (LTS) in different olfactory areas (Attems et al., 2014; Beach et al., 2009; Saito et al., 2016; Ubeda-Banon et al., 2010a,b, 2012). Furthermore, microstructural white matter reductions in the olfactory system, the reduction of the cholinergic centrifugal inputs to the OB, and the increased number of the dopaminergic cells observed in the OB have also been suggested as potential origins of smell loss (Ibarretxe-Bilbao et al., 2010; Mundinano et al., 2011, 2013).

PD and dementia with Lewy bodies are LBDs because of the presence of typical intracytoplasmic neuronal inclusions named Lewy bodies (LBs) together with Lewy neurites containing abnormal α-synuclein. Systematic study of cases with LB pathology has prompted a staging classification of PD (and LBDs) from the medulla oblongata and OB to the midbrain, diencephalic nuclei, and neocortex (Braak et al., 2002, 2003, 2004). Stages 1, 2, and 3 reflect,

* Corresponding author at: Proteomics Unit, Navarrabiomed, Biomedical Research Center, Instituto de Investigación Sanitaria de Navarra (IdiSNA), Pamplona, Spain. Tel.: +34 669879786; fax: +34 848422200.
E-mail address: esantamma@navarra.es (E. Santamaría).
[1] These authors share senior authorship.

https://doi.org/10.1016/j.neurobiolaging.2018.09.018

respectively, LB pathology in the medulla oblongata, pons, and midbrain; stage 4 includes, in addition, the basal prosencephalon and mesocortex; stage 5 extends to sensory association areas of the neocortex and prefrontal neocortex; and stage 6 includes, in addition, lesions in first-order sensory association areas of the neocortex and premotor areas (Braak et al., 2002, 2003, 2004). Similar categorization of LB pathology was used to classify dementia with Lewy bodies (McKeith et al., 1996, 2005, 2017). The later classification covers three stages: brain stem, limbic, and neocortical. Atypical cases not following a clear gradient of LB pathology from the lower brain stem and olfactory regions to the neocortex constitute about ten percent of total LBDs (Braak et al., 2006; Jellinger, 2008, 2009). The most frequent atypical LBD is the amygdala-predominant, which was added as a peculiar form to the former LBD-brain stem, LBD-limbic, and LBD-neocortical classification (Leverenz et al., 2008). All these classifications are based on the putative progression with time of LB pathology in the brain from the medulla oblongata and OB to the neocortex. Neuropathological studies have pointed out that the presence and severity of α-synuclein pathology in the OB reflect the presence and severity of synucleinopathy in other brain regions (Attems et al., 2014; Beach et al., 2009). Some studies have demonstrated that the presence of LTS in the OB predicts with 90% sensitivity and specificity the existence of neuropathologically confirmed PD (Beach et al., 2009). Moreover, the sensitivity and specificity of clinical olfactory testing in differentiating PD from non-PD range from 80% to 100% (Doty, 2012a). In addition, an OB atrophy and a significant reduction in olfactory performance have been detected in PD respect to control patients (Brodoehl et al., 2012; Li et al., 2016). In view of these clinical and neuropathological data, an in-depth molecular characterization of the OB neurodegeneration is necessary to reveal the missing links in the biochemical understanding of the early smell impairment in PD.

In this work, we applied mass spectrometry–based quantitative proteomics as a discovery platform to explore the magnitude and chronology of the OB proteome modulation across limbic, early-neocortical, and neocortical LTS stages in PD cases, also named LBD-limbic (LBDL) stage, LBD early-neocortical (LBDE) stage, and LBD neocortical (LBDN) stage. First, we have used a novel technique, called Matrix-Assisted Laser Desorption-Ionization Imaging Mass Spectrometry (MALDI-IMS), or MALDI imaging. The use of MALDI-IMS offers the great advantage to investigate the physiopathological changes taking place directly in tissues while retaining the histopathological context, enabling the so-called "molecular histology" (Caprioli et al., 1997; Chaurand et al., 2004). Second, we have applied a label-free shotgun proteomic approach getting more than 250 differentially expressed proteins between controls and PD-related phenotypes, pinpointing specific pathways, protein interaction networks, and potential novel therapeutic targets.

2. Materials and methods

2.1. Materials

The following reagents and materials were used: anti-glyceraldehyde 3-phosphate dehydrogenase (Calbiochem), anti-MKK3, anti-MKK6, anti-phospho MKK3 (Ser189)/MKK6 (Ser207), anti-p38 MAP kinase, anti-phospho p38 MAP kinase (Thr180/Tyr 182), anti-p38 MAPK alpha, anti-p38 MAPK beta, anti-PDK1, anti-phospho PDK1 (S241), anti-PKC-Pan, anti-phospho PKC-pan (T514), anti-pAkt (Ser473), anti-Akt, anti-pERK1/2 (Thr202/Tyr204), anti-ERK1/2 and anti-CACYBP (Cell Signaling), anti-CPNE6 (Thermo), anti-GNPDA2, anti-NEGR1, anti-RACK1, anti-SCGN (Abcam), anti-α-synuclein (Santa Cruz Biotech), and anti-DPP6 (Sigma). Electrophoresis reagents were purchased from Bio-Rad and trypsin from Promega.

2.2. Human samples

According to the Spanish Law 14/2007 of Biomedical Research, informed written consent forms were obtained for research purposes from relatives of patients included in this study. The study was conducted in accordance with the Declaration of Helsinki and all assessments, postmortem evaluations, and procedures were previously approved by the Clinical Ethics Committee of Navarra Health Service. OB specimens (Table 1), cerebrospinal fluid (CSF) samples (Additional file 7), and associated clinical and neuropathological data from patients with PD were supplied by the Parkinson's UK Brain Bank, funded by Parkinson's UK, a charity registered in England and Wales (258197) and in Scotland (SC037554), and the Neurological Tissue Bank from Navarrabiomed (Pamplona, Spain). Neuropathological assessment was performed according to standardized neuropathological scoring/grading systems (Alafuzoff et al., 2009). Twenty-one PD cases were distributed into LBDL (n = 7), LBDE (n = 6), and LBDN (n = 8) stages. Eight cases from elderly patients with no history or histological findings of any neurological disease were used as a control group. For validation and specificity analysis, OB specimens and associated neuropathological data from patients with AD (n = 14) were supplied by the Neurological Tissue Bank of the Biobank from the Hospital Clinic-Institut d'Investigacions Biomèdiques August Pi i Sunyer and the Neurological Tissue Bank of HUB-ICO-IDIBELL (Barcelona, Spain). All human brains considered in this study (n = 43) had a postmortem interval lower than 26 hours (Table 1). Serum samples and data from patients included in the study were provided by the Biobank of the University of Navarra and were processed following standard operating procedures approved by the ethical and scientific committees (Additional file 1).

2.3. MALDI imaging mass spectrometry

OBs from three different conditions were washed with phosphate-buffered saline and immediately frozen and stored at −80 °C until analyzed to preserve the native tissue morphology and minimize protein degradation. Sample tissues were sectioned at 14 μm using a Leica RM2235 cryostat (Leica, Wetzlar, DE) and thaw-mounted on indium-tin-oxide-coated glass slides (Bruker Daltonics, Bremen, DE) for mass spectrometry (MS) analysis, following previously published protocols (Lloro et al., 2017; Mourino-Alvarez et al., 2016).

2.4. Sample preparation for shotgun proteomics

OB specimens derived from control and PD cases were homogenized in a lysis buffer containing 7 M urea, 2 M thiourea, 4% (w/v) CHAPS, 50 mM DTT. The homogenates were spun down at 100.000 × *g* for 1 hour at 15 °C. Before proteomic analysis, protein extracts were precipitated with methanol/chloroform and pellets dissolved in 6M Urea and Tris 100 mM pH 7.8. Protein quantitation was performed with the Bradford assay kit (Bio-Rad).

2.5. Label-free LC-MS/MS

Protein enzymatic cleavage (10 μg) was carried out with trypsin (Promega; 1:20, w/w) at 37 °C for 16 hours as previously described (Shevchenko et al., 2006). Peptides mixtures were separated by a reversed-phase chromatography using an Eksigent NanoLC ultra 2D pump fitted with a 75 μm ID column (Eksigent 0.075 × 250). Samples were first loaded for desalting and concentration into a 0.5 cm length 100 μm ID precolumn packed with the same chemistry as the separating column. Mobile phases were 100% water and 0.1% formic acid (buffer A) and 100% acetonitrile and 0.1% formic acid (buffer B). Column gradient was developed in a 240-minute

Table 1
General characteristics of the patients included in the study

Case	Age	Sex	Clinical Diagnosis	Onset	Duration (y)	PMI (h)	Neuropathological Diagnosis
Controls							
C008	93	F				9	Aging-related changes
C048	68	M				10	Microvascular pathology
C064	63	F				21	Cerebellar infarcts
BK-0300	75	F				20	ARP I-II
BK-1378	78	M				6	Leucoencephalopathy
BK-1078	84	F				6	Vascular encephalopathy
BK-1195	82	F				8	Acute stroke
BK-1485	79	M				5	Acute stroke
PD							
PD295	83	M	PD	67	16	26	LBDL
PD340	67	M	PD	53	14	12	LBDL
PD356	86	F	PD	75	9	19	LBDL
PD541	72	M	PD	66	6	11	LBDL
PD546	84	F	PD	71	13	25	LBDL
PD579	76	M	PD	55	21	9	LBDL
PD591	77	M	PD	68	9	17	LBDL
PD275	79	M	PD	65	15	22	LBDE
PD354	88	F	PD	77	11	8	LBDE
PD423	66	F	PD	53	13	19	LBDE
PD436	90	M	PD	82	8	14	LBDE
PD520	80	M	PD	56	24	22	LBDE
PD530	85	M	PD	77	8	12	LBDE
PD357	71	M	PD	37	34	15	LBDN
PD450	66	M	PD	47	19	13	LBDN
PD495	88	F	PD	61	28	25	LBDN
PD501	89	F	PD	82	7	16	LBDN
PD537	84	M	PD	84	9	18	LBDN
PD550	83	F	PD	77	7	24	LBDN
PD562	79	M	PD	72	7	16	LBDN
PD636	84	M	PD	65	20	22	LBDN
AD							
1452	70	M	AD	n.a	n.a	3	Braak I
1370	79	F	AD	n.a	n.a	10	Braak II
1429	78	F	AD	n.a	n.a	3	Braak II
1433	62	M	AD	n.a	n.a	9	Braak II
1247	81	M	AD	n.a	n.a	5	Braak III
1517	84	M	AD	n.a	n.a	20	Braak III
1242	82	F	AD	n.a	n.a	17	Braak IV
1248	84	M	AD	n.a	n.a	12	Braak IV
1254	89	M	AD	n.a	n.a	3	Braak IV
CS-1445	73	F	AD	66	7	3	Braak VI
CS-0662	75	M	AD	71	4	4	Braak VI
CS-0535	81	F	AD	70	11	4	Braak VI
CS-0673	75	M	AD	60	15	4	Braak VI
CS-1232	84	M	AD	77	11	5	Braak VI

Key: AD, Alzheimer's disease; LBDL, LBD-limbic stage; LBDE, LBD early-neocortical stage; LBDN, LBD neocortical stage; PD, Parkinson's disease; PMI, postmortem interval.

two-step gradient from 5% B to 25% B in 210 minutes and 25% B to 40% B in 30 minutes. Eluting peptides were analyzed using a 5600 Triple-TOF system, as previously described (Lachen-Montes et al., 2017).

2.6. Peptide identification and quantification

MS/MS data acquisition, searching, peptide quantitation, and statistical analysis were performed as previously described (Lachen-Montes et al., 2017). MS raw data and search results files have been deposited to the ProteomeXchange Consortium (http://proteomecentral.proteomexchange.org) via the PRIDE partner repository (Vizcaino et al., 2014) with the data set identifiers PXD008036.

2.7. Statistical analysis

The statistical analysis used for the identification of differentially expressed proteins was performed using the Progenesis software and R scripts. Before applying any statistical test, data were submitted to several mathematical algorithms to remove the background, to align and compensate the "between-run variation," and to choose the same peaks in all samples in the peak-picking phase. Then, peptides were identified with the information obtained using Protein Pilot software. Output files with the identified proteins were then managed with R scripts for subsequent statistical analysis. One-way ANOVA test was applied to compare the results between all groups and unpaired Student's t-test was used for direct comparisons between two groups of samples. Statistical significance was set at $p < 0.05$ in all cases and 1% peptide false discovery rate threshold was considered (calculated based on the search results against a decoy database). In addition, an absolute fold change of <0.77 (downregulation) or >1.3 (upregulation) in linear scale was considered to be significantly differentially expressed. Concerning the immunoassays, the comparison made between the neuropathological groups and the neurological intact control group was performed using the unpaired t test for independent samples. A p value < 0.05 was considered significant. Results are represented as mean $\pm$ SE, and error bars show the standard error of the mean from the samples used in each group.

2.8. Bioinformatics

The proteomic information was analyzed using Reactome (Fabregat et al., 2018) to detect and infer differentially activated/deactivated pathways as a result of PD phenotypes. The identification of specifically dysregulated regulatory/metabolic networks across PD stages was analyzed through the use of QIAGEN's Ingenuity Pathway Analysis (QIAGEN Redwood City, www.qiagen.com/ingenuity).

2.9. Immunoblotting analysis

In the case of CSF samples, 100–150 μL was precipitated with four volumes of acetone o/n at −20 °C. Then, samples were centrifuged during 15 minutes at 14,000 rpm to obtain the protein pellet. Equal amounts of OB protein (10 μg) or CSF protein (8 μg) were resolved in 4%–15% TGX Stain-Free gels (Bio-Rad). Western blot analysis was performed as previously described (Lachen-Montes et al., 2017). After densitometric analyses (Image Lab Software Version 5.2; Bio-Rad), optical density values were expressed as arbitrary units and normalized to glyceraldehyde 3-phosphate dehydrogenase (tissue analysis) or to total stain in each gel lane (CSF analysis) (Moritz, 2017).

2.10. Enzyme-linked immunosorbent assay

Serum GNPDA2 concentrations were measured using enzyme-linked immunosorbent assay kits according to the manufacturer's instructions (MBS93411798; MyBioSource). The detection range was 0.62 ng/mL–20 ng/mL. Data were analyzed using GraphPad Prism software. Mann–Whitney *U* test was used for between-group comparisons. We considered *p*-value less than 0.05 to be statistically significant.

3. Results

3.1. Proteostasis impairment in the OB across LTS staging

In this work, we combined two complementary MS-based proteomic approaches such as MALDI-IMS and label-free quantitative proteomics to probe additional molecular disturbances in postmortem OBs dissected from clinically confirmed PD cases with respect to neurologically intact controls. First, MALDI-IMS was applied for the first time in the OB region to visualize in situ additional molecular disturbances between control and LB neuropathological stages (Fig. 1). Several masses with differential spatial distribution between control and LB stages have been found with receiving operating characteristic curves with statistical significance (area under the curve >0.8). To determine and characterize the progression and complexity of LTS-associated changes in this olfactory structure, the OB site-specific proteomic signature was monitored across LTS staging using a complementary label-free MS-based approach. Among 1629 quantified proteins across all experimental groups, 268 proteins tend to be differentially expressed between controls and PD phenotypes (Fig. 2A and Additional file 2). A progressive increment in OB monomeric α-synuclein protein levels was also evidenced across LTS stages by Western blot (Fig. 2B). Our analysis revealed that 148, 139, and 197 OB proteins are differentially expressed in the LBDL, LBDE, and LBDN stages, respectively. The distribution between upregulated and downregulated proteins was very similar across LTS grading (35%–40% downregulated, and 60%–65% upregulated proteins) (Fig. 2C). Interestingly, 65 OB proteins overlapped between all stages (Fig. 2D), suggesting a potential role during LTS progression in patients with PD. Most of these proteins mainly clustered in specific biological process like transport and RNA processing with specific molecular functions such as nucleotide binding and hydrolase activities (Additional file 3).

3.2. Olfactory dysregulated pathways across LTS grading

To extract biological knowledge, the differential OB proteome detected in each LTS stage was functionally categorized (Additional file 4). Immune system, metabolism of lipids, amino acids, and carbohydrates, signaling by growth factors and specific survival pathways, together with vesicle-mediated transport and axon guidance were the common over-represented dysregulated processes across LTS grading (Additional file 5A). To gain a more detailed description of the molecular mechanisms involved in the OB during LB pathology, subsequent analyses were performed to explore the differential olfactory proteome distributions across specific neuronal functionalities. As shown in Additional file 5B, our results point out a deregulation of specific protein clusters related to cell death, basal ganglia dysfunction, and movement disorders. Specifically, proteins involved in dyskinesia and tremor were exclusively mapped in the LBDN stage (Additional file 6). To characterize, in detail, the potential dysregulation of LTS-related protein interactomes in the OB during the neurodegenerative process, we have performed proteome-scale interaction networks merging the olfactory proteins that tend to be deregulated in each LTS stage. Using Ingenuity Pathway Analysis software, protein interactome maps have been constructed for each LTS stage (Fig. 3). In the LBDL stage, the functional interaction network indicated an alteration in HNRNP complexes (HNRNPA2B1, HNRNPM, HNRNPC, HNRNPH3, HNRNPR), RNA binding proteins (ILF2, MATR3, DDX6), as well as transcriptional and translational repressors (XRCC5, RACK1, RUVBL1) suggesting an impairment in RNA stability and pre-mRNA splicing processes (Fig. 3A). In the LBDE stage, the proteome-scale interaction network reflected an alteration in multiple interactors of nucleophosmin (NPM1), reinforcing the transcriptional derangements that occur at the level of the OB (Fig. 3B). The functional clustering also suggested an imbalance in signaling molecules involved in cell survival and differentiation such as CSNK2B, LIMS1, and PP2A (Fig. 3B). In the LBDN stage, functional interactors of specific survival routes were compromised, suggesting an imbalance in the survival potential of olfactory neurons (Fig. 3C).

3.3. Network-driven proteomics reveals olfactory derangements in survival pathways in PD

Signaling modulators like ERK, Akt, CaMKII, PKC, and p38 MAPK appeared as principal nodes in protein interactome maps (Fig. 3). Subsequent experiments were performed to monitor the activation state of this kinase panel across LTS staging. Respect to MAPK pathway, a significant increment in the steady-state levels of MEK was observed in the LBDN stage. On the contrary, a progressive downregulation of ERK levels was evidenced across LTS staging (Fig. 4A). Phosphoinositide-dependent protein kinase 1 (PDK1) activity depends on the autophosphorylation on Ser241, activating PKC signal transduction (Mora et al., 2004). Despite the upregulation in total PDK1 levels observed in the LBDL stage, PDK1 was inactivated across the LBDE and LBDN stages (Fig. 4B). Moreover, PDK1 inactivation was accompanied by a decrease in the activation status of PKC isoforms in the LBDE stage, as revealed by Western blot using a specific pan-antibody against phosphorylated PKC isoforms (Fig. 4B). MKK3 and MKK6 are dual-specificity protein kinases that activate p38 MAPK (Derijard et al., 1995). We evaluated the activation state of olfactory MKK3-6/p38 MAPK axis across LTS staging. As shown in Fig. 4C, MKK3/6 were significantly inactivated across all stages, mainly due to a drop in total MKK6 levels. On the other hand, no significant changes were observed in the activation

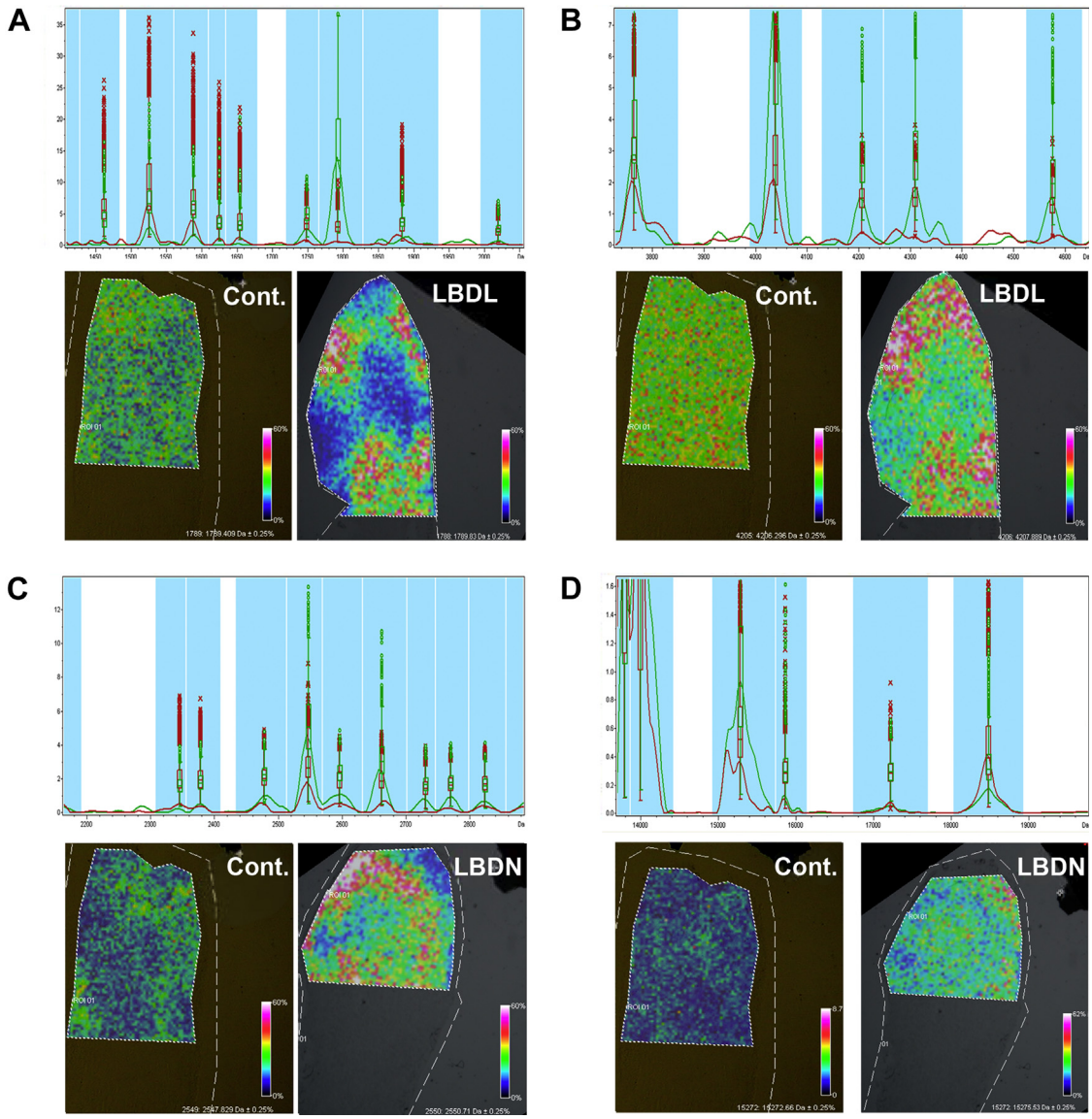

Fig. 1. MALDI imaging mass spectrometry of human OB. Mean spectra of the whole section of control OB (red) and each LTS stages (green) and the corresponding spatial distribution of the selected peaks. (A) band at 1789 Th. (B) band at 4205 Th. (C) band at 2549 Th, and (D) band at 15,272 Th. This pattern can also be shown in the corresponding whisker-plots. Abbreviations: OB, olfactory bulb; LTS, Lewy-type alpha-synucleinopathies; LBDL, LBD-limbic stage; MALDI, Matrix-Assisted Laser Desorption-Ionization Imaging Mass Spectrometry. (For interpretation of the references to color in this figure legend, the reader is referred to the Web version of this article.)

state of p38 MAPK, detecting an overexpression of p38-alpha and -beta subunits in the LBDL stage and a specific increment of p38-alpha protein in the LBDN stage (Fig. 4C). These data suggest the existence of upstream disruption of olfactory MAPK, PDK1/PKC, and MKK3-6/p38 MAPK axis among neuropathological stages. On the other hand, a slight increment in the activation state of Akt and CaMKII was observed in the LBDL stage, although these changes were not statistically significant (Fig. 4D).

3.4. Searching common pathological olfactory substrates in AD and PD phenotypes

The potential existence of common olfactory pathological substrates in AD and PD, mainly due to the equivalent severe olfactory deficits present at earliest stages of both neurological syndromes, has been recently proposed (Doty, 2012b, 2017). With the aim to identify common olfactory protein intermediates deregulated in both neurodegenerative backgrounds, a cross-disease study of selected olfactory molecules was performed in sporadic AD cases. For that, OB samples derived from low (Braak I-II), intermediate (Braak III-IV), and high AD (Braak V-VI) were included in the cross-disease study (Table 1). The selection of assessing the protein panel for verification was based primarily on (1) differential expression across LTS stages and novelty in human PD pathophysiology (SCGN, CACYBP, GNPDA2, RACK1) and (2) differential expression in the OB from different neurological disorders (CPNE6 and DPP6) (Zelaya et al., 2015). Our group has previously identified CPNE6 (Copine-6) and DPP6 (Dipeptidyl aminopeptidase-like protein 6) as olfactory protein mediators deregulated in specific neurological syndromes (Zelaya et al., 2015). As shown in Fig. 4E, olfactory CPNE6 and DPP6 protein levels were significantly increased in the LBDL and LBDN stages. Secretagogin (SCGN) is a calcium-binding protein considered a marker of periglomerular and deep-layer olfactory interneurons (Attems et al., 2012). Calcyclin-binding protein (CACYBP) is involved in cytoskeletal dynamics and in the regulation of transcriptional responses in neurons (Filipek et al., 2008; Kilanczyk et al., 2015). Glucosamine 6

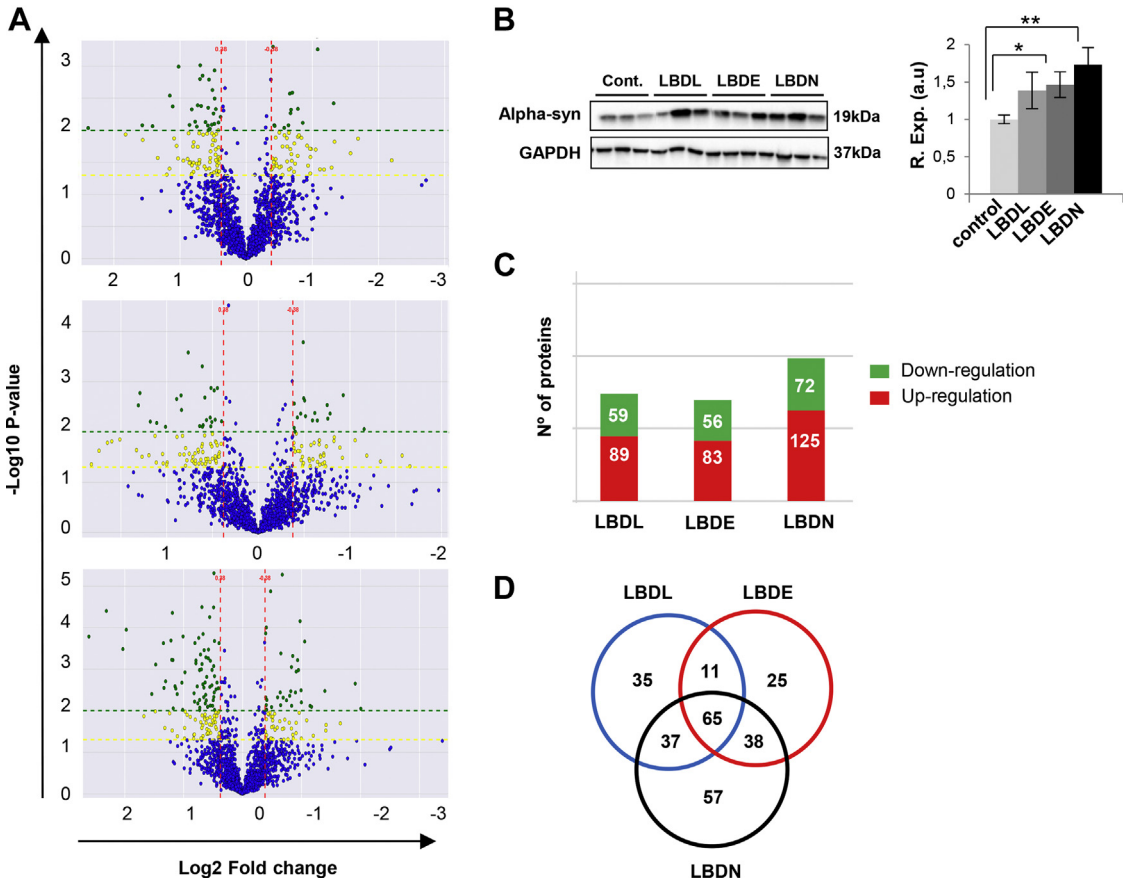

Fig. 2. OB differentially expressed proteins across PD-related phenotypes. (A) Volcano plots from the pairwise comparisons: control versus LBDL stage (upper panel), LBDE stage (middle panel), and LBDN stage (lower panel). Differential proteins: $p < 0.01$ in green, and $p < 0.05$ in yellow. (B) OB monomeric α-synuclein expression. (C) Differential olfactory proteome distributions. (D) Common and unique differential proteins between LTS stages. $^{*}p < 0.05$ versus control group; $^{**}p < 0.01$ versus control group. Abbreviations: OB, olfactory bulb; PD, Parkinson's disease; LBDL, LBD-limbic stage; LBDE, LBD early-neocortical stage; LBDN, LBD neocortical stage; LTS, Lewy-type alpha-synucleinopathies. (For interpretation of the references to color in this figure legend, the reader is referred to the Web version of this article.)

phosphate isomerase 2 (GNPDA2) participates in the glucose metabolism, converting D-glucosamine-6-phosphate into D-fructose-6-phosphate and ammonium (Arreola et al., 2003). Receptor of activated protein C kinase 1 (RACK1) protects neurons from oxidative stress–induced apoptosis (Ma et al., 2014). First, and with the aim to complement and partially validate our proteomic workflow, the steady-state levels of our protein panel were checked across LTS staging by Western blotting. In accordance with our proteomic findings, the immunoblots confirmed the olfactory overexpression of SCGN, GNPDA2, and RACK1 across LTS stages (Fig. 4F). In addition, a significant downregulation of CACYBP was observed in the LBDE and LBDN stages (Fig. 4F). The monitorization of the expression of our protein panel in the OB from AD cases (Fig. 5A) revealed that (1) SCGN protein levels were downregulated in the OB derived from high AD cases, (2) CACYBP was specifically overexpressed in low AD cases, (3) a significant increment in OB GNPDA2 protein levels across low and intermediate AD, (4) no significant changes in OB RACK1 were observed across AD staging. This cross-disease analysis revealed the existence of common protein intermediates that are differentially deregulated during PD and AD progression at the level of the OB.

3.5. GNPDA2 protein biofluid profile differs between controls and patients with PD

We further examined whether our protein panel could be detected in the CSF of patients with PD and ultimately serves as potential novel PD biomarkers. Interestingly, GNPDA2 was previously characterized by mass spectrometry in CSF (Guldbrandsen et al., 2014). Subsequent experiments were performed to check the GNPDA2 expression in the CSF of PD patients (n = 16) and healthy control patients (n = 9) (Additional file 7) by Western blot analysis. As shown in Fig. 5B, GNPDA2 protein levels were significantly increased in CSF in patients PD respect to controls, showing an inverse correlation between GNPDA2 and α-synuclein protein levels detected in CSF. However, serum GNPDA2 levels were decreased in PD population (Fig. 6) (Additional file 1), suggesting that the GNPDA2 profiles observed in both biofluids may be a consequence of the damaged blood-brain barrier (BBB) previously observed in PD (Sweeney et al., 2018).

4. Discussion

In view of the general recognition that olfactory dysfunction is an early feature of PD, we consider that the elucidation of the progressive proteome-wide alterations that occur in the OB might provide novel candidate proteins for a druggability assessment in PD. Neuroproteomics has been successfully applied to discover novel protein mediators associated with PD pathogenesis, diagnosis, and evolution (Jin et al., 2006; Lehnert et al., 2012; Licker et al., 2012, 2014; Liu et al., 2015). To our knowledge, this is the first study to characterize potential PD-associated molecular changes in the human OB combining imaging mass spectrometry

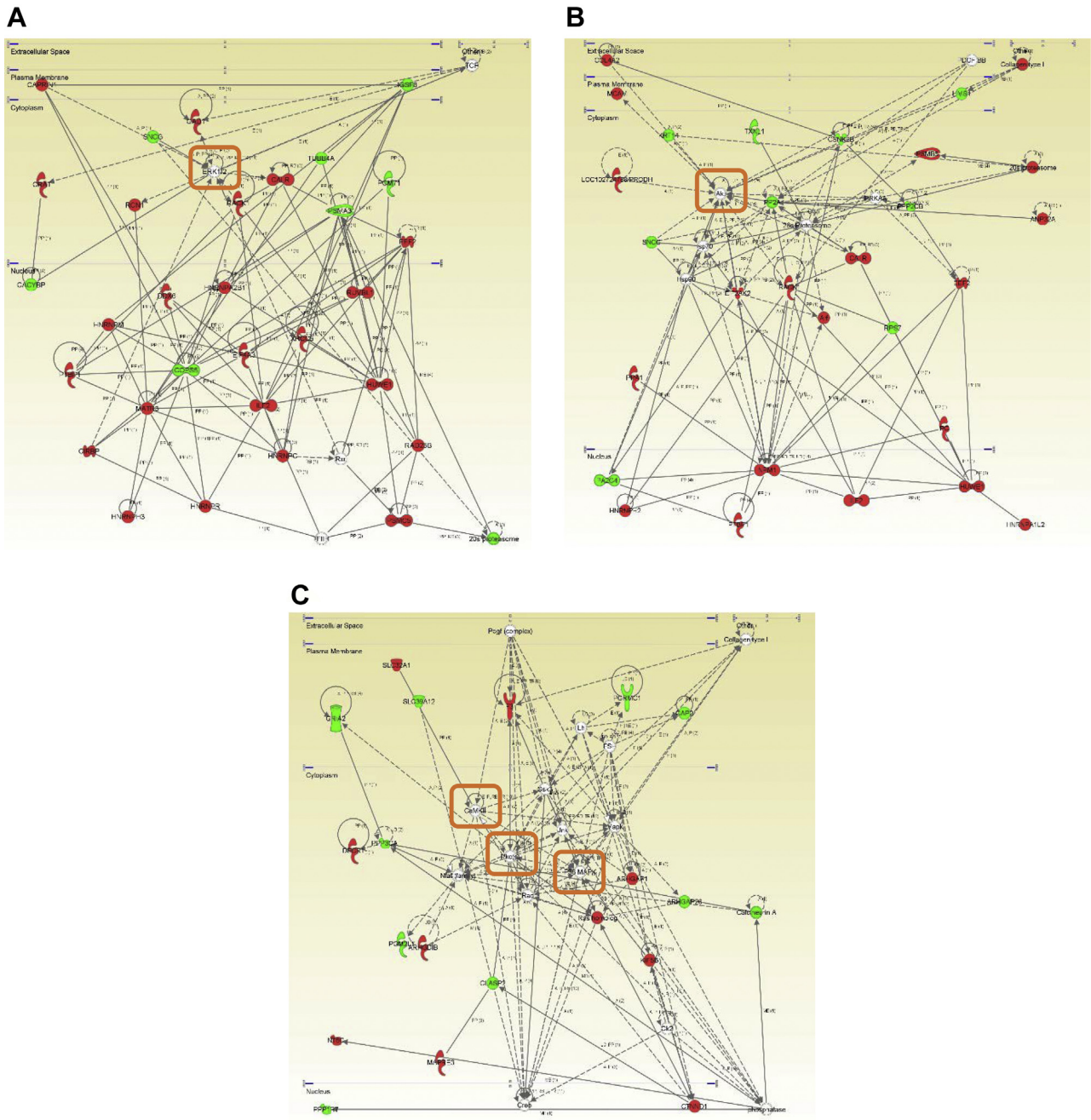

Fig. 3. Protein interactome maps for differentially expressed proteins in the OB during LTS progression. Visual representation of the relationships detected in LBDL (A), LBDE (B), and LBDN (C). Upregulated proteins in red and downregulated proteins in green. Complete legend in http://ingenuity.force.com/ipa/articles/Feature_Description/Legend. Abbreviations: OB, olfactory bulb; LBDL, LBD-limbic stage; LBDE, LBD early-neocortical stage; LBDN, LBD neocortical stage; LTS, Lewy-type alpha-synucleinopathies. (For interpretation of the references to color in this figure legend, the reader is referred to the Web version of this article.)

and quantitative proteomics. In a first approach, using MALDI-IMS as a molecular histology technique, we have observed that there are obvious molecular changes between control and LB stages, at protein level, with several distinctive masses (receiving operating characteristic curves with area under the curve values >0.8) adopting marked positional domains in LB stages. Our data suggest that MALDI-IMS is a suitable approach that complements current neuropathological classifications. Some of the differential expressed OB proteins detected across LTS stages have been proposed as α-synuclein interactors or protein components of LB inclusions (Betzer et al., 2015; Leverenz et al., 2007): IGSF8 (in LBDL stage), GNAO1, OMG, ARPC5, and NIPSNAP1 (in LBDE stage), HSD17B10, ATP6V1D, PGRMC1, ACADS, and TUBB2 (in LBDN stage), VPS53 (common to LBDL and LBDE stages), ATP1A2, EHD1, EEF1A2, and BANF1 (common to LBDE and LBDN stages), and TUBB4A, TPPP, and TUBA4A (common to all stages). To establish a functional relationship between the OB and other PD-affected regions at the proteome level, a traceability analysis was performed comparing the differential OB protein set with respect to deregulated proteins previously detected in functionally related structures such as the substantia nigra, striatum, and cortex derived from patients with PD (Licker et al., 2014; Riley et al., 2014). In accordance with downregulated OB proteome, the expression of five nigral proteins, three cortical proteins, and striatal protein OMG were also

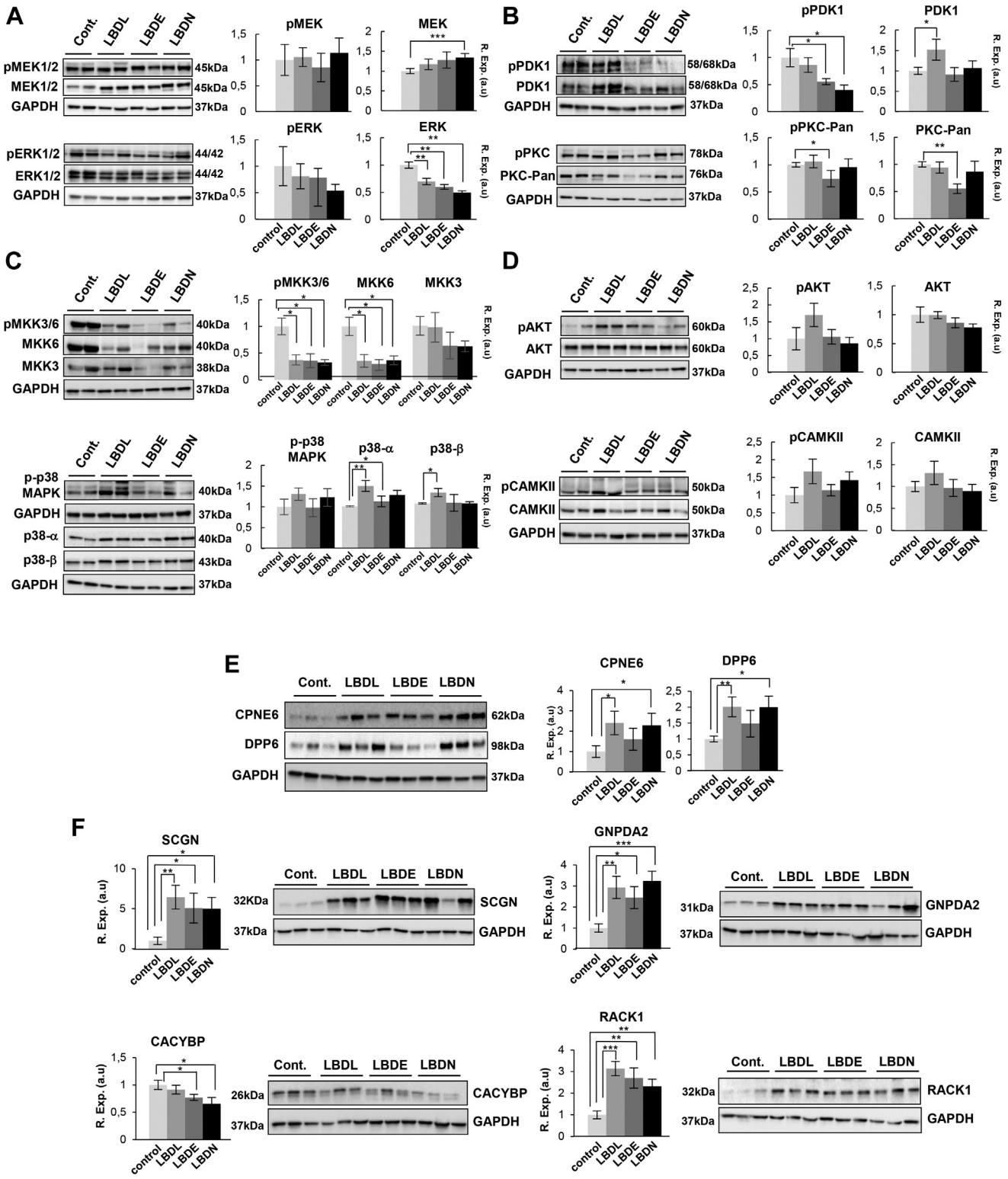

Fig. 4. Monitoring of OB survival routes and specific protein intermediates across LTS grading. Levels and phosphorylation of MAP kinases (A), PDK1/PKC (B), MKK3-6/p38 MAPK (C), and AKT and CaMKII kinases (D) in the OB across PD phenotypes. CPNE6 and DPP6 protein expression levels across LTS stages (E). Protein variation in SCGN, CACYBP, GNPDA2, and RACK1 levels across PD phenotypes (F). *$p < 0.05$ versus control group; ** $p < 0.01$ versus control group; *** $p < 0.001$ versus control group. Statistical analysis between LTS stages is shown in additional file 9A. Abbreviations: CACYBP, calcyclin-binding protein; GNPDA2, glucosamine 6 phosphate isomerase 2; LBDL, LBD-limbic stage; LBDE, LBD early-neocortical stage; LBDN, LBD neocortical stage; LTS, Lewy-type alpha-synucleinopathies; OB, olfactory bulb; PD, Parkinson's disease; SCGN, Secretagogin; RACK1; Receptor of activated protein C kinase 1.

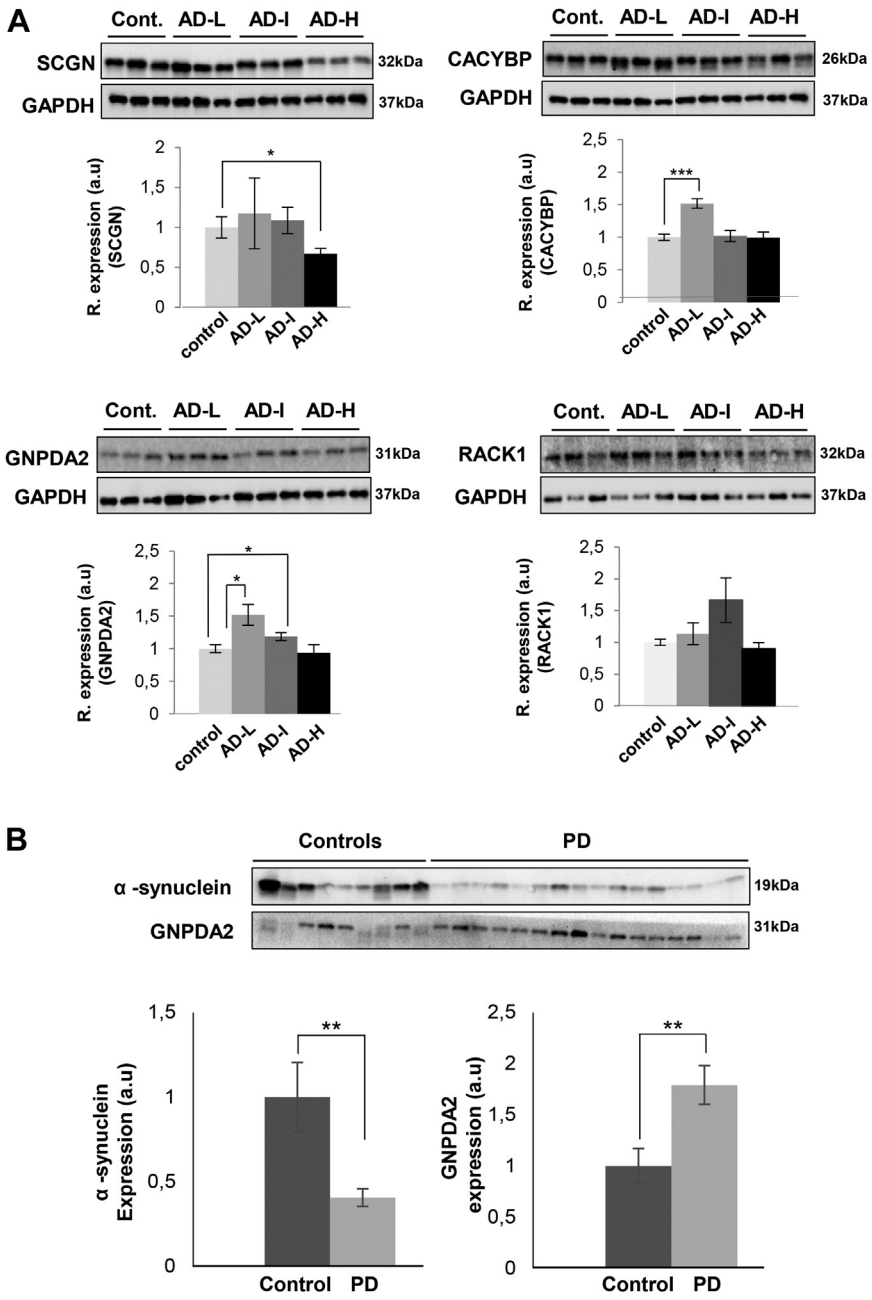

Fig. 5. Monitoring of specific olfactory proteins during AD progression. GNPDA2 and α-synuclein levels in the CSF of patients with PD. (A) Protein levels of SCGN, CACYBP, GNPDA2, and RACK1 were monitored by Western blotting across AD stages. Statistical analysis between AD stages is shown in additional file 9B. (B) Inverse correlation between GNPDA2 and α-synuclein protein expression in CSF from patients with PD. $^{*}p < 0.05$ versus control group; $^{**}p < 0.01$ versus control group; $^{***}p < 0.01$ versus control group. Abbreviations: AD, Alzheimer's disease; CACYBP, calcyclin-binding protein; CSF, cerebrospinal fluid; GNPDA2, glucosamine 6 phosphate isomerase 2; PD, Parkinson's disease; RACK1; Receptor of activated protein C kinase 1.

downmodulated in PD. In contrast, nigral protein MYO6, fourteen striatal proteins, and eighteen cortical proteins present an opposite expression pattern (upregulation) in patients with PD (Additional file 8). With respect to the upregulated OB proteome, four nigral proteins, twenty striatal proteins, and seventeen cortical proteins were also upregulated in the PD phenotypes (Additional file 8). This information suggests that the coordinated deregulation of specific protein modules shared among brain areas might explain, in part, the existence of conserved transcriptional programs that may be activated/deactivated across structures during PD pathogenesis.

The aberrant regulation of a subset of kinases may represent the triggering events leading to the spread of an abnormal signaling in PD (Wang et al., 2012). In this context, cell survival mechanisms have been proposed as targets for neuroprotective strategies in delay onset or slow progression of PD (Goswami et al., 2017). Analyzing the signaling interactions predicted by our network system biology approach, we determine potential upstream regulators highly interconnected with deregulated olfactory proteins. An increment in phospho-ERK levels has been previously reported in midbrain dopaminergic neurons in PD brains (Zhu et al., 2002, 2003). However, in leukocytes, ERK1/2 activity does not significantly differ between controls and patients with PD (White et al., 2007). In our case, the activation of the prosurvival factor ERK1/2 tends to be compromised across the LTS stages. Interestingly, a

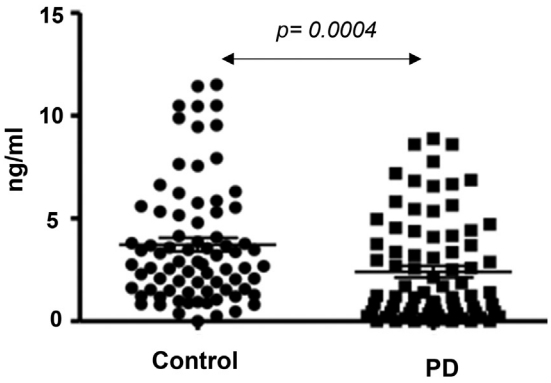

Fig. 6. Serum GNPDA2 levels in PD population. GNPDA2 levels were measured in the sera derived from 164 individuals (82 controls; mean age: 69 years; 51 M/31 F and 82 patients with PD: mean age: 67 years; 41 M/41 F) by ELISA (Mann-Whitney *U* test; *p*-value: 0.0004). Abbreviations: ELISA, enzyme-linked immunosorbent assay; GNPDA2, glucosamine 6 phosphate isomerase 2; PD, Parkinson's disease.

hyperactivation of upstream MEK1/2 and ERK1/2 was evidenced in the OB derived from patients with AD (Lachen-Montes et al., 2016), suggesting that MAPK signaling clearly differs between PD and AD phenotypes at olfactory level. It has been shown that p38 MAPK is activated by α-synuclein (Rannikko et al., 2015), being localized in neurons of PD brain stem bearing LBs or α-synuclein deposits (Ferrer et al., 2001). An early inactivation of MKK3/6-p38 MAPK axis has been observed in initial AD stages at OB level, recovering normal levels in intermediate and advanced AD stages (Lachen-Montes et al., 2017). However, a distinct profile was observed in PD phenotypes. The inactivation of MKK3/6 across LTS stages suggests the involvement of other kinase-based route in the apparent maintenance of olfactory p38 MAPK activity in the OB from PD. To our knowledge, our data represent the first molecular link between PDK1 dysregulation and PD. An impairment of olfactory PDK1/PKC signaling axis was observed in LBDL and LBDE stages. Interestingly, and in line with these findings, this pathway is also modified in the OB of patients with AD (Lachen-Montes et al., 2017). As α-synuclein specifically downregulates PKCδ isoform in dopaminergic cells (Jin et al., 2011), further work will be necessary to clarify the specific role of each PKC isoform in olfactory neurons during PD progression.

Although the activation state of specific olfactory survival pathways differs between PD and AD, this study has allowed the identification of a subset of common protein intermediates in the OB from patients with PD and AD with respect to nondemented controls, suggesting that these shared proteins might participate as common pathological substrates during the olfactory neurodegenerative process in both neurological disorders (Doty, 2012b, 2017). However, it is important to note that 14 of 21 (67%) patients with PD included in our study present concomitant AD-type tau pathology (Braak stage I-II) (data not shown). Having said that, we cannot exclude the possibility that the shared differential OB proteome observed between AD and PD may be due to the AD concomitant pathology present in patients with PD. In the present study, novel common mediators have emerged but with different expression profiling between PD and AD phenotypes, emphasizing the importance of neuropathological stage–dependent analysis in the search of potential olfactory therapeutic targets. CPN6 and DPP6 tend to be upregulated in the OB from patients with PD, indicating specific differences in spine plasticity and synaptic function (Lin et al., 2013; Reinhard et al., 2016) with respect to AD (Zelaya et al., 2015). Moreover, the different expression profile observed between the AD and LTS stages for SCGN, CACYBP, and RACK1 proteins also points out subtle differences in calcium fluxes, cytoskeletal dynamics, and oxidative response in the OB from patients with AD and PD. Interestingly, the metabolic enzyme GNPDA2 was overexpressed in most PD and AD cases (see also Additional file 9B), showing an inverse correlation between GNPDA2 and α-synuclein protein levels in the CSF from patients with PD. However, serum GNPDA2 levels were significantly decreased in PD population. The different protein profile across fluids has been also observed for other proteins in the context of PD such as complement C4, serotransferrin, apolipoprotein AI, haptoglobin, zinc-alpha-2-glycoprotein, apolipoprotein E, beta-2-glycoprotein, ceruloplasmin, complement C3, and serum albumin (Halbgebauer et al., 2016). The lack of standardization between laboratories in CSF collection and preparation procedures may be a reason for this type of observation. However, from a biological point of view, these molecular events may be due to the damage of the blood-brain barrier observed in patients with PD (Alexander et al., 1994; Kortekaas et al., 2005; Sweeney et al., 2018). Checking the Human Protein Atlas (Uhlen et al., 2010) (www.proteinatlas.org), GNPDA2 is highly expressed by the brain (https://www.proteinatlas.org/ENSG00000163281-GNPDA2/tissue), so additional experiments are needed to explain the GNPDA2 efflux, rates, and transportation (both the brain-to-blood and the blood-to-brain directions) in the PD pathophysiology. Being aware of the small number of cases assessed in this study, the novel relation of secreted GNPDA2 and α-synuclein should be further evaluated in combination with other biochemical markers to improve the current diagnostic assays (Eusebi et al., 2017; Forland et al., 2018).

5. Conclusion

Overall, the present study provides new insights regarding the molecular mechanisms governing the olfactory dysfunction occurring during PD progression. Besides the pathological depositions of α-synuclein occurring at the level of the OB, we have demonstrated a clear disarrangement in the olfactory proteostasis, affecting cell survival routes and showing potential common pathological substrates between PD and AD. Moreover, the application of high-throughput proteomic approaches again proves to be a useful tool to decipher the proteome expression profiles in olfactory structures and more importantly to define potential fluid biomarkers for the diagnosis of neurodegenerative processes.

Disclosure statement

The authors declare that they have no competing interests.

Acknowledgements

The authors are very grateful to the patients who generously donated the brain tissue or fluid samples for research purposes. The authors thank the collaboration of Parkinson's UK Brain Bank funded by Parkinson's UK, a charity registered in England and Wales (258197) and in Scotland (SC037554), the Neurological Tissue Bank of the Biobank from the Hospital Clinic-Institut d'Investigacions Biomédiques August Pi i Sunyer (IDIBAPS, Barcelona), the Neurological Tissue Bank of HUB-ICO-IDIBELL (Barcelona, Spain), the Neurological Tissue Bank of Navarrabiomed (Pamplona, Spain), and the Biobank of the University of Navarra for providing us the OB specimens, CSF, and serum samples as well as the associated clinical and neuropathological data. The authors want to kindly thank Ellen Gelpi (Neurological Tissue Bank, IDIBAPS) for her help. The Proteomics Unit of Navarrabiomed is a member of ProteoRed and PRB3-ISCIII and is supported by grant PT17/0019, of the PE I+D+i 2013-2016, funded by ISCIII and ERDF. The Clinical Neuroproteomics Laboratory of Navarrabiomed is a member of the Spanish Network

of Olfaction (ROE). This project is part of the HUPO Brain Proteome Project, and these results are lined up with the Spanish Initiative on the Human Proteome Project (SpHPP).

This work was funded by grants from the Spanish Ministry of Economy and Competitiveness (MINECO) (Ref. SAF2014-59340-R), Department of Economic Development from Government of Navarra (Ref. PC023-PC024, PC025, PC081-82 and PI059) and Obra Social la Caixa to ES. AG-M was supported by PEJ-2014-A-61949 (MINECO). ML-M was supported by a predoctoral fellowship from the Public University of Navarra (UPNA).

Authors' contribution: JF-I and ES designed and supervised the complete study. ML-M and AG-M performed proteomic experiments, bioinformatics analysis, protein validation and signaling pathway characterizations. II and FE performed MALDI-IMS experiments. IF and DG performed neuropathological classifications. JF-I and ES performed mass spectrometry analysis and data interpretation. ES wrote the article. All authors reviewed the article.

MS raw data and search results files have been deposited to the ProteomeXchange Consortium (http://proteomecentral.proteomexchange.org) via the PRIDE partner repository with the data set identifiers PXD008036 (for reviewers: username: reviewer45850@ebi.ac.uk; password: hBK0q6GD).

Appendix A. Supplementary data

Supplementary data to this article can be found online at https://doi.org/10.1016/j.neurobiolaging.2018.09.018.

References

Alafuzoff, I., Ince, P.G., Arzberger, T., Al-Sarraj, S., Bell, J., Bodi, I., Bogdanovic, N., Bugiani, O., Ferrer, I., Gelpi, E., Gentleman, S., Giaccone, G., Ironside, J.W., Kavantzas, N., King, A., Korkolopoulou, P., Kovacs, G.G., Meyronet, D., Monoranu, C., Parchi, P., Parkkinen, L., Patsouris, E., Roggendorf, W., Rozemuller, A., Stadelmann-Nessler, C., Streichenberger, N., Thal, D.R., Kretzschmar, H., 2009. Staging/typing of Lewy body related alpha-synuclein pathology: a study of the BrainNet Europe Consortium. Acta Neuropathol. 117, 635–652.

Alexander, G.M., Schwartzman, R.J., Grothusen, J.R., Gordon, S.W., 1994. Effect of plasma levels of large neutral amino acids and degree of parkinsonism on the blood-to-brain transport of levodopa in naive and MPTP parkinsonian monkeys. Neurology 44, 1491–1499.

Arreola, R., Valderrama, B., Morante, M.L., Horjales, E., 2003. Two mammalian glucosamine-6-phosphate deaminases: a structural and genetic study. FEBS Lett. 551, 63–70.

Attems, J., Alpar, A., Spence, L., McParland, S., Heikenwalder, M., Uhlen, M., Tanila, H., Hokfelt, T.G., Harkany, T., 2012. Clusters of secretagogin-expressing neurons in the aged human olfactory tract lack terminal differentiation. Proc. Natl. Acad. Sci. U S A 109, 6259–6264.

Attems, J., Walker, L., Jellinger, K.A., 2014. Olfactory bulb involvement in neurodegenerative diseases. Acta Neuropathol. 127, 459–475.

Baba, T., Kikuchi, A., Hirayama, K., Nishio, Y., Hosokai, Y., Kanno, S., Hasegawa, T., Sugeno, N., Konno, M., Suzuki, K., Takahashi, S., Fukuda, H., Aoki, M., Itoyama, Y., Mori, E., Takeda, A., 2012. Severe olfactory dysfunction is a prodromal symptom of dementia associated with Parkinson's disease: a 3 year longitudinal study. Brain 135 (Pt 1), 161–169.

Beach, T.G., White 3rd, C.L., Hladik, C.L., Sabbagh, M.N., Connor, D.J., Shill, H.A., Sue, L.I., Sasse, J., Bachalakuri, J., Henry-Watson, J., Akiyama, H., Adler, C.H., 2009. Olfactory bulb alpha-synucleinopathy has high specificity and sensitivity for Lewy body disorders. Acta Neuropathol. 117, 169–174.

Betzer, C., Movius, A.J., Shi, M., Gai, W.P., Zhang, J., Jensen, P.H., 2015. Identification of synaptosomal proteins binding to monomeric and oligomeric alpha-synuclein. PLoS One 10, e0116473.

Braak, H., Del Tredici, K., Bratzke, H., Hamm-Clement, J., Sandmann-Keil, D., Rub, U., 2002. Staging of the intracerebral inclusion body pathology associated with idiopathic Parkinson's disease (preclinical and clinical stages). J. Neurol. 249 (Suppl 3), III/1-5.

Braak, H., Del Tredici, K., Rub, U., de Vos, R.A., Jansen Steur, E.N., Braak, E., 2003. Staging of brain pathology related to sporadic Parkinson's disease. Neurobiol. Aging 24, 197–211.

Braak, H., Ghebremedhin, E., Rub, U., Bratzke, H., Del Tredici, K., 2004. Stages in the development of Parkinson's disease-related pathology. Cell Tissue Res 318, 121–134.

Braak, H., Muller, C.M., Rub, U., Ackermann, H., Bratzke, H., de Vos, R.A., Del Tredici, K., 2006. Pathology associated with sporadic Parkinson's disease–where does it end? J. Neural. Transm. Suppl. 89–97.

Brodoehl, S., Klingner, C., Volk, G.F., Bitter, T., Witte, O.W., Redecker, C., 2012. Decreased olfactory bulb volume in idiopathic Parkinson's disease detected by 3.0-tesla magnetic resonance imaging. Mov. Disord. 27, 1019–1025.

Caprioli, R.M., Farmer, T.B., Gile, J., 1997. Molecular imaging of biological samples: localization of peptides and proteins using MALDI-TOF MS. Anal. Chem. 69, 4751–4760.

Chaurand, P., Schwartz, S.A., Billheimer, D., Xu, B.J., Crecelius, A., Caprioli, R.M., 2004. Integrating histology and imaging mass spectrometry. Anal. Chem. 76, 1145–1155.

Derijard, B., Raingeaud, J., Barrett, T., Wu, I.H., Han, J., Ulevitch, R.J., Davis, R.J., 1995. Independent human MAP-kinase signal transduction pathways defined by MEK and MKK isoforms. Science 267, 682–685.

Doty, R.L., 2008. The olfactory vector hypothesis of neurodegenerative disease: is it viable? Ann. Neurol. 63, 7–15.

Doty, R.L., 2012a. Olfaction in Parkinson's disease and related disorders. Neurobiol. Dis. 46, 527–552.

Doty, R.L., 2012b. Olfactory dysfunction in Parkinson disease. Nat. Rev. Neurol. 8, 329–339.

Doty, R.L., 2017. Olfactory dysfunction in neurodegenerative diseases: is there a common pathological substrate? Lancet Neurol. 16, 478–488.

Eusebi, P., Giannandrea, D., Biscetti, L., Abraha, I., Chiasserini, D., Orso, M., Calabresi, P., Parnetti, L., 2017. Diagnostic utility of cerebrospinal fluid alpha-synuclein in Parkinson's disease: a systematic review and meta-analysis. Mov. Disord. 32, 1389–1400.

Fabregat, A., Jupe, S., Matthews, L., Sidiropoulos, K., Gillespie, M., Garapati, P., Haw, R., Jassal, B., Korninger, F., May, B., Milacic, M., Roca, C.D., Rothfels, K., Sevilla, C., Shamovsky, V., Shorser, S., Varusai, T., Viteri, G., Weiser, J., Wu, G., Stein, L., Hermjakob, H., D'Eustachio, P., 2018. The reactome pathway knowledgebase. Nucleic Acids Res. 46, D649–D655.

Ferrer, I., Blanco, R., Carmona, M., Puig, B., Barrachina, M., Gomez, C., Ambrosio, S., 2001. Active, phosphorylation-dependent mitogen-activated protein kinase (MAPK/ERK), stress-activated protein kinase/c-Jun N-terminal kinase (SAPK/JNK), and p38 kinase expression in Parkinson's disease and Dementia with Lewy bodies. J. Neural Transm. (Vienna) 108, 1383–1396.

Filipek, A., Schneider, G., Mietelska, A., Figiel, I., Niewiadomska, G., 2008. Age-dependent changes in neuronal distribution of CacyBP/SIP: comparison to tubulin and the tau protein. J. Neural Transm. (Vienna) 115, 1257–1264.

Forland, M.G., Ohrfelt, A., Dalen, I., Tysnes, O.B., Blennow, K., Zetterberg, H., Pedersen, K.F., Alves, G., Lange, J., 2018. Evolution of cerebrospinal fluid total alpha-synuclein in Parkinson's disease. Parkinsonism Relat. Disord. 49, 4–8.

Goswami, P., Joshi, N., Singh, S., 2017. Neurodegenerative signaling factors and mechanisms in Parkinson's pathology. Toxicol. In Vitro 43, 104–112.

Guldbrandsen, A., Vethe, H., Farag, Y., Oveland, E., Garberg, H., Berle, M., Myhr, K.M., Opsahl, J.A., Barsnes, H., Berven, F.S., 2014. In-depth characterization of the cerebrospinal fluid (CSF) proteome displayed through the CSF proteome resource (CSF-PR). Mol. Cell Proteomics 13, 3152–3163.

Halbgebauer, S., Ockl, P., Wirth, K., Steinacker, P., Otto, M., 2016. Protein biomarkers in Parkinson's disease: focus on cerebrospinal fluid markers and synaptic proteins. Mov. Disord. 31, 848–860.

Ibarretxe-Bilbao, N., Junque, C., Marti, M.J., Valldeoriola, F., Vendrell, P., Bargallo, N., Zarei, M., Tolosa, E., 2010. Olfactory impairment in Parkinson's disease and white matter abnormalities in central olfactory areas: a voxel-based diffusion tensor imaging study. Mov. Disord. 25, 1888–1894.

Jellinger, K.A., 2008. A critical reappraisal of current staging of Lewy-related pathology in human brain. Acta Neuropathol. 116, 1–16.

Jellinger, K.A., 2009. A critical evaluation of current staging of alpha-synuclein pathology in Lewy body disorders. Biochim. Biophys. Acta 1792, 730–740.

Jin, H., Kanthasamy, A., Ghosh, A., Yang, Y., Anantharam, V., Kanthasamy, A.G., 2011. alpha-Synuclein negatively regulates protein kinase Cdelta expression to suppress apoptosis in dopaminergic neurons by reducing p300 histone acetyltransferase activity. J. Neurosci. 31, 2035–2051.

Jin, J., Hulette, C., Wang, Y., Zhang, T., Pan, C., Wadhwa, R., Zhang, J., 2006. Proteomic identification of a stress protein, mortalin/mthsp70/GRP75: relevance to Parkinson disease. Mol. Cell Proteomics 5, 1193–1204.

Kilanczyk, E., Filipek, A., Hetman, M., 2015. Calcyclin-binding protein/Siah-1-interacting protein as a regulator of transcriptional responses in brain cells. J. Neurosci. Res. 93, 75–81.

Klingelhoefer, L., Reichmann, H., 2015. Pathogenesis of Parkinson disease–the gut-brain axis and environmental factors. Nat. Rev. Neurol. 11, 625–636.

Kortekaas, R., Leenders, K.L., van Oostrom, J.C., Vaalburg, W., Bart, J., Willemsen, A.T., Hendrikse, N.H., 2005. Blood-brain barrier dysfunction in parkinsonian midbrain in vivo. Ann. Neurol. 57, 176–179.

Lachen-Montes, M., Gonzalez-Morales, A., de Morentin, X.M., Perez-Valderrama, E., Ausin, K., Zelaya, M.V., Serna, A., Aso, E., Ferrer, I., Fernandez-Irigoyen, J., Santamaria, E., 2016. An early dysregulation of FAK and MEK/ERK signaling pathways precedes the beta-amyloid deposition in the olfactory bulb of APP/PS1 mouse model of Alzheimer's disease. J. Proteomics 148, 149–158.

Lachen-Montes, M., Gonzalez-Morales, A., Zelaya, M.V., Perez-Valderrama, E., Ausin, K., Ferrer, I., Fernandez-Irigoyen, J., Santamaria, E., 2017. Olfactory bulb neuroproteomics reveals a chronological perturbation of survival routes and a disruption of prohibitin complex during Alzheimer's disease progression. Sci. Rep. 7, 9115.

Lehnert, S., Jesse, S., Rist, W., Steinacker, P., Soininen, H., Herukka, S.K., Tumani, H., Lenter, M., Oeckl, P., Ferger, B., Hengerer, B., Otto, M., 2012. iTRAQ and multiple reaction monitoring as proteomic tools for biomarker search in cerebrospinal fluid of patients with Parkinson's disease dementia. Exp. Neurol. 234, 499–505.

Leverenz, J.B., Hamilton, R., Tsuang, D.W., Schantz, A., Vavrek, D., Larson, E.B., Kukull, W.A., Lopez, O., Galasko, D., Masliah, E., Kaye, J., Woltjer, R., Clark, C., Trojanowski, J.Q., Montine, T.J., 2008. Empiric refinement of the pathologic assessment of Lewy-related pathology in the dementia patient. Brain Pathol. 18, 220–224.

Leverenz, J.B., Umar, I., Wang, Q., Montine, T.J., McMillan, P.J., Tsuang, D.W., Jin, J., Pan, C., Shin, J., Zhu, D., Zhang, J., 2007. Proteomic identification of novel proteins in cortical lewy bodies. Brain Pathol. 17, 139–145.

Li, J., Gu, C.Z., Su, J.B., Zhu, L.H., Zhou, Y., Huang, H.Y., Liu, C.F., 2016. Changes in olfactory bulb volume in Parkinson's disease: a systematic review and meta-analysis. PLoS One 11, e0149286.

Licker, V., Cote, M., Lobrinus, J.A., Rodrigo, N., Kovari, E., Hochstrasser, D.F., Turck, N., Sanchez, J.C., Burkhard, P.R., 2012. Proteomic profiling of the substantia nigra demonstrates CNDP2 overexpression in Parkinson's disease. J. Proteomics 75, 4656–4667.

Licker, V., Turck, N., Kovari, E., Burkhardt, K., Cote, M., Surini-Demiri, M., Lobrinus, J.A., Sanchez, J.C., Burkhard, P.R., 2014. Proteomic analysis of human substantia nigra identifies novel candidates involved in Parkinson's disease pathogenesis. Proteomics 14, 784–794.

Lin, L., Sun, W., Throesch, B., Kung, F., Decoster, J.T., Berner, C.J., Cheney, R.E., Rudy, B., Hoffman, D.A., 2013. DPP6 regulation of dendritic morphogenesis impacts hippocampal synaptic development. Nat. Commun. 4, 2270.

Liu, Y., Zhou, Q., Tang, M., Fu, N., Shao, W., Zhang, S., Yin, Y., Zeng, R., Wang, X., Hu, G., Zhou, J., 2015. Upregulation of alphaB-crystallin expression in the substantia nigra of patients with Parkinson's disease. Neurobiol. Aging 36, 1686–1691.

Lloro, I., Fernandez-Irigoyen, J., Escobes, I., Azkargorta, M., Santamaria, E., Elortza, F., 2017. Methods for human olfactory bulb tissue studies using peptide/protein MALDI-TOF imaging mass spectrometry. In: Santamaria, E., Fernandez-Irigoyen, J. (Eds.), Neuromethods. Humana Press, New York, NY, pp. 91–106.

Ma, J., Wu, R., Zhang, Q., Wu, J.B., Lou, J., Zheng, Z., Ding, J.Q., Yuan, Z., 2014. DJ-1 interacts with RACK1 and protects neurons from oxidative-stress-induced apoptosis. Biochem. J. 462, 489–497.

McKeith, I.G., Boeve, B.F., Dickson, D.W., Halliday, G., Taylor, J.P., Weintraub, D., Aarsland, D., Galvin, J., Attems, J., Ballard, C.G., Bayston, A., Beach, T.G., Blanc, F., Bohnen, N., Bonanni, L., Bras, J., Brundin, P., Burn, D., Chen-Plotkin, A., Duda, J.E., El-Agnaf, O., Feldman, H., Ferman, T.J., Ffytche, D., Fujishiro, H., Galasko, D., Goldman, J.G., Gomperts, S.N., Graff-Radford, N.R., Honig, L.S., Iranzo, A., Kantarci, K., Kaufer, D., Kukull, W., Lee, V.M.Y., Leverenz, J.B., Lewis, S., Lippa, C., Lunde, A., Masellis, M., Masliah, E., McLean, P., Mollenhauer, B., Montine, T.J., Moreno, E., Mori, E., Murray, M., O'Brien, J.T., Orimo, S., Postuma, R.B., Ramaswamy, S., Ross, O.A., Salmon, D.P., Singleton, A., Taylor, A., Thomas, A., Tiraboschi, P., Toledo, J.B., Trojanowski, J.Q., Tsuang, D., Walker, Z., Yamada, M., Kosaka, K., 2017. Diagnosis and management of dementia with Lewy bodies: fourth consensus report of the DLB Consortium. Neurology 89, 88–100.

McKeith, I.G., Dickson, D.W., Lowe, J., Emre, M., O'Brien, J.T., Feldman, H., Cummings, J., Duda, J.E., Lippa, C., Perry, E.K., Aarsland, D., Arai, H., Ballard, C.G., Boeve, B., Burn, D.J., Costa, D., Del Ser, T., Dubois, B., Galasko, D., Gauthier, S., Goetz, C.G., Gomez-Tortosa, E., Halliday, G., Hansen, L.A., Hardy, J., Iwatsubo, T., Kalaria, R.N., Kaufer, D., Kenny, R.A., Korczyn, A., Kosaka, K., Lee, V.M., Lees, A., Litvan, I., Londos, E., Lopez, O.L., Minoshima, S., Mizuno, Y., Molina, J.A., Mukaetova-Ladinska, E.B., Pasquier, F., Perry, R.H., Schulz, J.B., Trojanowski, J.Q., Yamada, M., 2005. Diagnosis and management of dementia with Lewy bodies: third report of the DLB Consortium. Neurology 65, 1863–1872.

McKeith, I.G., Galasko, D., Kosaka, K., Perry, E.K., Dickson, D.W., Hansen, L.A., Salmon, D.P., Lowe, J., Mirra, S.S., Byrne, E.J., Lennox, G., Quinn, N.P., Edwardson, J.A., Ince, P.G., Bergeron, C., Burns, A., Miller, B.L., Lovestone, S., Collerton, D., Jansen, E.N., Ballard, C., de Vos, R.A., Wilcock, G.K., Jellinger, K.A., Perry, R.H., 1996. Consensus guidelines for the clinical and pathologic diagnosis of dementia with Lewy bodies (DLB): report of the consortium on DLB international workshop. Neurology 47, 1113–1124.

Mora, A., Komander, D., van Aalten, D.M., Alessi, D.R., 2004. PDK1, the master regulator of AGC kinase signal transduction. Semin. Cell Dev. Biol. 15, 161–170.

Moritz, C.P., 2017. Tubulin or not tubulin: heading toward total protein staining as loading control in western blots. Proteomics 17.

Mourino-Alvarez, L., Iloro, I., de la Cuesta, F., Azkargorta, M., Sastre-Oliva, T., Escobes, I., Lopez-Almodovar, L.F., Sanchez, P.L., Urreta, H., Fernandez-Aviles, F., Pinto, A., Padial, L.R., Akerstrom, F., Elortza, F., Barderas, M.G., 2016. MALDI-Imaging Mass Spectrometry: a step forward in the anatomopathological characterization of stenotic aortic valve tissue. Sci. Rep. 6, 27106.

Mundinano, I.C., Caballero, M.C., Ordonez, C., Hernandez, M., DiCaudo, C., Marcilla, I., Erro, M.E., Tunon, M.T., Luquin, M.R., 2011. Increased dopaminergic cells and protein aggregates in the olfactory bulb of patients with neurodegenerative disorders. Acta Neuropathol. 122, 61–74.

Mundinano, I.C., Hernandez, M., Dicaudo, C., Ordonez, C., Marcilla, I., Tunon, M.T., Luquin, M.R., 2013. Reduced cholinergic olfactory centrifugal inputs in patients with neurodegenerative disorders and MPTP-treated monkeys. Acta Neuropathol. 126, 411–425.

Rannikko, E.H., Weber, S.S., Kahle, P.J., 2015. Exogenous alpha-synuclein induces toll-like receptor 4 dependent inflammatory responses in astrocytes. BMC Neurosci. 16, 57.

Reinhard, J.R., Kriz, A., Galic, M., Angliker, N., Rajalu, M., Vogt, K.E., Ruegg, M.A., 2016. The calcium sensor Copine-6 regulates spine structural plasticity and learning and memory. Nat. Commun. 7, 11613.

Rey, N.L., Steiner, J.A., Maroof, N., Luk, K.C., Madaj, Z., Trojanowski, J.Q., Lee, V.M., Brundin, P., 2016. Widespread transneuronal propagation of alpha-synucleinopathy triggered in olfactory bulb mimics prodromal Parkinson's disease. J. Exp. Med. 213, 1759–1778.

Riley, B.E., Gardai, S.J., Emig-Agius, D., Bessarabova, M., Ivliev, A.E., Schule, B., Alexander, J., Wallace, W., Halliday, G.M., Langston, J.W., Braxton, S., Yednock, T., Shaler, T., Johnston, J.A., 2014. Systems-based analyses of brain regions functionally impacted in Parkinson's disease reveals underlying causal mechanisms. PLoS One 9, e102909.

Saito, Y., Shioya, A., Sano, T., Sumikura, H., Murata, M., Murayama, S., 2016. Lewy body pathology involves the olfactory cells in Parkinson's disease and related disorders. Mov. Disord. 31, 135–138.

Shevchenko, A., Tomas, H., Havlis, J., Olsen, J.V., Mann, M., 2006. In-gel digestion for mass spectrometric characterization of proteins and proteomes. Nat. Protoc. 1, 2856–2860.

Sweeney, M.D., Sagare, A.P., Zlokovic, B.V., 2018. Blood-brain barrier breakdown in Alzheimer disease and other neurodegenerative disorders. Nat. Rev. Neurol. 14, 133–150.

Ubeda-Banon, I., Saiz-Sanchez, D., de la Rosa-Prieto, C., Argandona-Palacios, L., Garcia-Munozguren, S., Martinez-Marcos, A., 2010a. alpha-Synucleinopathy in the human olfactory system in Parkinson's disease: involvement of calcium-binding protein- and substance P-positive cells. Acta Neuropathol. 119, 723–735.

Ubeda-Banon, I., Saiz-Sanchez, D., de la Rosa-Prieto, C., Martinez-Marcos, A., 2012. alpha-Synuclein in the olfactory system of a mouse model of Parkinson's disease: correlation with olfactory projections. Brain Struct. Funct. 217, 447–458.

Ubeda-Banon, I., Saiz-Sanchez, D., de la Rosa-Prieto, C., Mohedano-Moriano, A., Fradejas, N., Calvo, S., Argandona-Palacios, L., Garcia-Munozguren, S., Martinez-Marcos, A., 2010b. Staging of alpha-synuclein in the olfactory bulb in a model of Parkinson's disease: cell types involved. Mov. Disord. 25, 1701–1707.

Uhlen, M., Oksvold, P., Fagerberg, L., Lundberg, E., Jonasson, K., Forsberg, M., Zwahlen, M., Kampf, C., Wester, K., Hober, S., Wernerus, H., Bjorling, L., Ponten, F., 2010. Towards a knowledge-based human protein Atlas. Nat. Biotechnol. 28, 1248–1250.

Vizcaino, J.A., Deutsch, E.W., Wang, R., Csordas, A., Reisinger, F., Rios, D., Dianes, J.A., Sun, Z., Farrah, T., Bandeira, N., Binz, P.A., Xenarios, I., Eisenacher, M., Mayer, G., Gatto, L., Campos, A., Chalkley, R.J., Kraus, H.J., Albar, J.P., Martinez-Bartolome, S., Apweiler, R., Omenn, G.S., Martens, L., Jones, A.R., Hermjakob, H., 2014. ProteomeXchange provides globally coordinated proteomics data submission and dissemination. Nat. Biotechnol. 32, 223–226.

Wang, G., Pan, J., Chen, S.D., 2012. Kinases and kinase signaling pathways: potential therapeutic targets in Parkinson's disease. Prog. Neurobiol. 98, 207–221.

White, L.R., Toft, M., Kvam, S.N., Farrer, M.J., Aasly, J.O., 2007. MAPK-pathway activity, Lrrk2 G2019S, and Parkinson's disease. J. Neurosci. Res. 85, 1288–1294.

Zelaya, M.V., Perez-Valderrama, E., de Morentin, X.M., Tunon, T., Ferrer, I., Luquin, M.R., Fernandez-Irigoyen, J., Santamaria, E., 2015. Olfactory bulb proteome dynamics during the progression of sporadic Alzheimer's disease: identification of common and distinct olfactory targets across Alzheimer-related co-pathologies. Oncotarget 6, 39437–39456.

Zhu, J.H., Guo, F., Shelburne, J., Watkins, S., Chu, C.T., 2003. Localization of phosphorylated ERK/MAP kinases to mitochondria and autophagosomes in Lewy body diseases. Brain Pathol. 13, 473–481.

Zhu, J.H., Kulich, S.M., Oury, T.D., Chu, C.T., 2002. Cytoplasmic aggregates of phosphorylated extracellular signal-regulated protein kinases in Lewy body diseases. Am. J. Pathol. 161, 2087–2098.